AADE-13-FTCE-26

Visco-Elastic Settling Rate Models to Determine Sag Potential of Non-Aqueous Drilling Fluids

Sandeep D. Kulkarni, Sharath Savari, Anita Gantepla, Robert Murphy, Dale Jamison, Narongsak Tonmukayakul and Kushabhau Teke, Halliburton.

Abstract

One of less-understood phenomena in invert-emulsion non-aqueous drilling fluids (NAF) is *sag* that leads to unwanted density variations. Sag is considered to be a static as well as dynamic phenomenon and can become severe for highly deviated/complex wells. To understand and tackle this issue, there has been need for experimental techniques and empirical methods to predict sag for different well environments and fluid compositions.

A method for quantitatively determining the solids settling rate in a NAF under shear is presented in this paper. The method is based on empirical equation which is a modified form of Stoke's Law that considers effects of viscous as well as elastic properties of NAF on solids settling rate. For building and validating the empirical equation, viscosity is measured using conventional oilfield viscometers while the elastic properties of fluid under shear in form of the first normal stress difference N_1 are measured using an advanced rheometer. This is combined with experimental data on solids settling rate *U(mm/hr)* in NAF obtained from using the Dynamic High Angle Sag Tester (DHAST^{TM}) instrument at specified conditions of temperature, pressure and shear rate.

A method to make an accurate determination of sag in the field has been an unresolved need for a long time. This method may be used readily for accurate solids settling rate predictions using the rheology data under relevant conditions of temperature, pressure and shear. The model could serve as a handy tool to mud engineers to evaluate the sag behavior at given well conditions and to make speedy decisions at the rig site to optimize fluid formulations for sag management.

Introduction

The barite sag or weight material sag phenomenon is defined most appropriately by the API Work Group 3, formed under the aegis of API 13D subcommittee[1], as follows: "Weight-material sag is recognized by a significant (> 0.5lbm/gal) mud density variation, lighter followed by heavier than the nominal mud density, measured when circulating bottoms up where a weighted mud has remained uncirculated for a period of time in a directional well". Mud weight variations have been reported to be in the range of 1.0 – 1.5 ppg. Both the drilling fluid properties and drilling operational parameters play significant roles and require appropriate monitoring/maintenance in controlling barite sag.

In the present work, the feasibility of modeling weighting material (or barite) sag or sedimentation behavior based on rheological properties of the non-aqueous drilling fluids (NAF) is investigated. As the drilling fluids are known to have significant elastic properties[2], the selected sag models in this work include an additional term in the Stokes-drag equation that captures the effect of elasticity of the drilling fluid.

.

Visco-elastic Settling Rate Models

The particle sedimentation in Newtonian and non-Newtonian fluids has been studied extensively in the literature. As barite sag is known to happen at static or low shear conditions, it could is described by Stokes flow conditions (*Re* << 1). For Stokes regime, the drag force on a spherical particle in a Newtonian fluid is described by

$$F_d = 6\pi\eta a \mathrm{U} \qquad (\text{for } \mathrm{Re} < 0.1) \text{.....(1)}$$

where η is fluid viscosity, a is particle radius and U is rate of sedimentation.

If the sphere is allowed to fall from rest in a viscous medium, it will reach a "terminal" (or steady) velocity state. The overall force acting on the particle is zero at this state, i.e., the drag force on a spherical particle, is balanced by the net gravitational force acting on the sphere: for a spherical particle settling in a Newtonian fluid under stokes flow condition, the force balance is described by the following equation:[3]

$$\frac{4}{3}\pi a^3(\rho_s - \rho_f)\mathrm{g} = 6\pi\eta a \mathrm{U} \text{.....(2)}$$

where ρ_s and ρ_f are densities of the particle and surrounding fluid respectively.

However, for sedimentation of particles in non-Newtonian fluids, **Equation 2** needs to be modified to account for the fluid properties like yield stress and visco-elasticity. For the present investigation, the barite sag or sedimentation in a continuously sheared system appears to be influenced mainly by viscous as well as elastic properties of the drilling fluid.

The drag on a sphere in visco-elastic fluids is determined by a complex interplay between the shear and extensional rheological characteristics of the system.[3] In highly visco-elastic fluids, drag enhancement has been observed

experimentally by many researchers.[5,6] Attempts have been made to explain the drag factor using steady shear properties including shear viscosity and first normal stress difference (N_1) in the case of highly elastic Boger fluids.[7] Recently Tonmukayakul and Morris[8,9] suggested the following equation to capture the sedimentation in visco-elastic fluids; this equation provides an additional term incorporated into Equation 2.

$$\frac{4}{3}\pi a^3(\rho_s - \rho_f)g \approx 6\pi a \eta(\dot{\gamma})U(\dot{\gamma}) + \alpha f[N_1(\dot{\gamma})] \ldots (3)$$

where α is an dimensionless empirical constant and N_1 is the first normal stress difference of the fluid under steady shear.

Note that the rheological parameters, fluid viscosity (η) and N_1 are dependent on the shear rate ($\dot{\gamma}$) applied to the drilling fluid and hence the sedimentation rate also becomes dependent on the rate at which fluid is being sheared. In the present work, **Equation 3** will be used as a basis to model the sag behavior of barite particles in the NAFs.

The experimental data needed for the barite sag model was obtained from different instruments: Viscosity (η) from FANN® 35 viscometer; fluid elasticity or N_1 from an advanced rheometer; and the sag rates from the Dynamic High Angle Sag Tester (DHAST) instrument. Work performed using the DHAST instrument has been presented earlier[10,11] and to our knowledge, it is by far one of the best instruments available in the industry to predict weight material sag in drilling under the given conditions of temperature, pressure and shear rates.

The experimental data obtained was incorporated in the selected sag model so as to build the model, i.e., to obtain the dimensionless constants in the model equation. Once the dimensionless constants (e.g., α) were obtained, the model predicted sag rates for unknown fluids (not used for building the model) using rheological information (η and N_1) as input. It was found that the developed model predicts sag rates for unknown fluids with reasonable accuracy. Thus, it was demonstrated that an empirical model for predicting barite sedimentation/sag rate could be built based on rheological characteristics of the drilling fluid.

Methodology and Experimental Procedures

Drilling Fluids Formulations

Non-aqueous drilling fluids (NAF) were formulated with commercially available mineral base oils, invert emulsifiers, lime, polymeric viscosifiers, high-pressure high-temperature (HPHT) filtration control agent, sized calcium carbonate (mean particle size 5 microns) and barite. Twelve NAFs were formulated such as to have a variation in the base oil type, additive concentration, oil/water ratio (OWR), and mud weight as shown in **Appendix 1**. The formulated drilling fluids were conditioned at 150°F for 16 hours before performing the tests.

FANN® 35 Viscometer Rheology

The standard oilfield FANN 35 viscometer rheology of the drilling fluids (after hot-rolling) was measured at 150°F. This viscometer provides stress measurements (or dial readings) for 600, 300, 200, 100, 6 and 3 rpm rotational speeds from which the standard PV, YP and LSYP values were calculated. The FANN 35 data for all the selected muds has been tabulated in **Appendix 2**.

Normal Stress Measurements

Using an advanced rheometer from Anton Paar (MCR-301), rotational and oscillatory rheology of a fluid can be measured for a wide range of shear rate/stress and temperature for different geometries. In the present study, "parallel plate geometry (50 *mm* diameter)" was used to study the rotational rheology of the mud system. The gap between the parallel plates was chosen to be 1 mm. All the tests were conducted at temperature of 150°F and atmospheric pressure.

The drilling fluid (after hot-rolling) was mixed in a multi-mixer for about 10 minutes and then the well-mixed drilling fluid was added between the parallel plates of the PP-50 geometry (~ 2 ml). The drilling fluid was pre-sheared between the plates for 1 min at the shear rate of 10 s^{-1}. Then, the drilling fluid was subjected to shear ramp starting from 0.1 s^{-1} to a maximum shear rate of 50 s^{-1} with 50 data points collected at each of the selected intermediate shear rates. The shear and normal stress response was recorded for every data point. The N_1 data on all the selected drilling fluids has been tabulated in **Appendix 3**.

Significance of normal stress: When a visco-elastic material is deformed there are not only one-dimensional forces or stresses acting in the direction of deformation. In fact, a state of three dimensional deformations (3*3 tensor) always exists for a visco-elastic material. The tensor consists of three normal stress components τ_{xx}, τ_{yy}, τ_{zz}. For most visco-elastic materials, the τ_{xx} component shows the highest value of the all three normal stresses. The first normal stress difference is stated as: $N_1 = \tau_{xx} - \tau_{yy}$.

The magnitude of N_1 is a measure of the degree of fluid visco-elasticity which would be zero for a visco-inelastic fluid. As used herein, the magnitude of N_1 is the absolute value of N_1 and may be expressed as $|N_1|$. When N_1 is measured with parallel plate geometry of an advanced rheometer, the negative value of N_1 implies that the rheometer plates are pulled together, as observed in the present work. Here, it is demonstrated that the N_1 values for drilling fluids, as determined from the Anton Paar rheometer, influence the sedimentation or sag rate of barite particles.

Dynamic Sag Testing

The DHAST unit measures the sag potential of a drilling fluid in terms of settling rates (*mm/hr*) under dynamic shear conditions and at elevated temperatures and pressures. It consists of a tube which is filled with the test sample (drilling fluid) and set at an angle of 45° from vertical, an angle which is known to cause severe barite sag conditions in the field.

Inside the tube, there is a rotating shaft which shears the sample for inducing dynamic conditions. The gap between the rotating shaft and the inside wall of tube is small and generates shear rates equivalent to 0.35 times the RPM of shaft. The desired pressure is applied on the fluid sample and the tube is heated to maintain the desired temperature.

As the experiment begins with a uniform drilling fluid, when the barite settles, the center of mass of the tube changes. The force required to maintain the tube in the equilibrium position is measured in terms of an electrical signal. As more and more barite settles, the amount of power required to keep the tube in equilibrium also increases. Finally, this power is converted into the settling rate of barite. Thus, as output, the DHAST instrument provides sag potential of the fluid in terms of the solids settling rate *U* in mm/hr.

Sample parameters like density, OWR, salt concentration, and type of base oil would be required as input for estimating the settling rate. In the present work, the pressure (*P*) on the fluid is 2000 psi while the temperature (*T*) is 150°F. A shear rate of ≈ 5 s^{-1} is applied. The measured settling rate is averaged over a period of 3 hr. after achieving temperature stability in the experiment. The averaged settling/sag rate is reasonably considered to be a characteristic of the fluid with initial uniform suspension.

Results and Discussion

The NAF samples used in this work had variations in the base oil type, viscosifier concentration/type, OWR, mud weight and low gravity solids (LGS) content as shown Appendix 1.

After hot-rolling or conditioning, the drilling fluids were tested to obtain experimental data for building the model. The tests include rheology measurements (FANN 35 viscometer viscosity and N_1) and DHAST unit measurements by following procedures described in the earlier section. In the present work, the focus would be only on modeling the barite settling rate when the fluid undergoes shearing motion of ~ 5 s^{-1} (as it is typically the lowest shear rate condition that could generated using a standard oilfield FANN 35 viscometer). Thus, the rheology data obtained only at the chosen shear rate condition would be used for modeling purposes for eight different drilling fluids (**Table 1**). Also, as mentioned earlier, only the sag rate obtained in the first three hours after warm-up of DHAST unit measurements (at $\dot{\gamma} \approx 5\, s^{-1}$) would be considered for the purpose of modeling. The corresponding data is shown in Table 1.

Table 1: Experimental data on rheology and sag rates for fluids I to VIII (Temperature = 150°F).

Drilling Fluid No.	FANN 35 $\Theta_{3\,\mathrm{RPM}}(lb/100\,ft^2)$ $[\dot{\gamma} \approx 5\, s^{-1}]$	$\lvert N_1 \rvert$ (Pa) $[\dot{\gamma} \approx 5\, s^{-1}]$	Expt. U_{avg} (mm/hr) [from DHAST] $[\dot{\gamma} \approx 5\, s^{-1}]$
Fluid-I	10	130	4.71
Fluid-II	6	235	5.55
Fluid-III	15	110	4.31
Fluid-IV	13	325	2.48
Fluid-V	8	244	3.78
Fluid-VI	11	233	3.43
Fluid-VII	7	240	3.8
Fluid-VIII	11	150	3.93

Evaluation of Empirical Constants and Model Optimization

Here, Equation 3 was applied in a form to include a non-linear dependence on N_1 that could characterize the nature of relation between sag and fluid elasticity in a quantitative manner. The non-linear dependence was captured by the parameter "β" in **Equation 4** shown below:

$$\frac{4}{3}\pi\, a_i^3(\rho_s - \rho_f)g \approx 6\pi\, a_i\, \eta(\dot{\gamma}) U_i(\dot{\gamma}) + \alpha(4\pi a_i^2 N_1{}^{\beta}(\dot{\gamma})) \qquad .....(4)$$

For accurate predictions, the wide range of particle size distribution of barite is taken into account by dividing the entire particle size range into smaller intervals as shown in **Appendix 4**; then Equation 4 was applied separately to each interval with mean size (a_i) to determine settling rate of particles of corresponding size denoted as U_i.

The volume fraction of a size interval with mean size a_i in the PSD distribution curve (Appendix 4) is denoted as (ψ_i). Thus, the average sedimentation rate of barite particles is estimated as:

$$U_{avg} = \sum \psi_i\, U_i \qquad .....(5)$$

The obtained experimental data on η, $|N_1|$ and sag rate U_{avg} (at $\dot{\gamma} \approx 5\, s^{-1}$) for different drilling fluids mentioned in Table 1 is incorporated in the above **Equations 4** and **5.** The viscosity η is evaluated from Table 1 as

$$\eta = \frac{\Theta_{3RPM}}{\dot{\gamma}} \text{ where } \dot{\gamma} \approx 5\, s^{-1}.$$

The barite density is incorporated as ρ_s = *4.2 g/cc* and the fluid density ρ_f was represents the base oil being used. Using these input data, Equations 4 and 5 were solved to empirically obtain values of the constants "α" and "*β*".

Now, with the empirically obtained value of "α" and "*β*", the model was ready for application. Using the empirical constants along with fluid rheology (η and N_1), sag rate (U_{avg}) could be predicted from the sag model, i.e., Equations 4 and 5. The model-based sag rate predictions for the drilling fluids I to VIII were in excellent agreement with corresponding experimental sag rates as shown in **Figure 1**. The RMSE (Root Mean Square Error) between the predicted and measured values of sag rates (U) was found to be only around 0.492 mm/hr; this error was equivalent to the instrumental error expected for the DHAST instrument. In other words, the predicted rates are within ±10% of the corresponding experimental values.

Figure 2 shows a map of sag rate prediction (using the empirically obtained α and *β*) as a function of 3-RPM FANN Viscometer 35 readings, Θ_{3RPM} , at various values of $|N_1|$. The figure clearly indicates that the sag rate is sensitive to both fluid viscosity and elasticity of the drilling fluid. As expected, the sag rate decreases with increase in viscosity (i.e., 3 RPM FANN 35 dial reading, Θ_{3RPM}). In addition, the figure indicates that as $|N_1|$ increases, the sag rate decreases; this behavior suggests that the fluid elasticity resists the rate of sedimentation under Stokes flow conditions which is similar to the observations by Tonmukayakul and Morris. The above results show that the built model certainly has potential to predict sag rates with reasonable accuracy; however, it is important to check the validity of the model for some of the unseen drilling fluids (drilling fluids that are not used for obtaining the empirical model parameters).

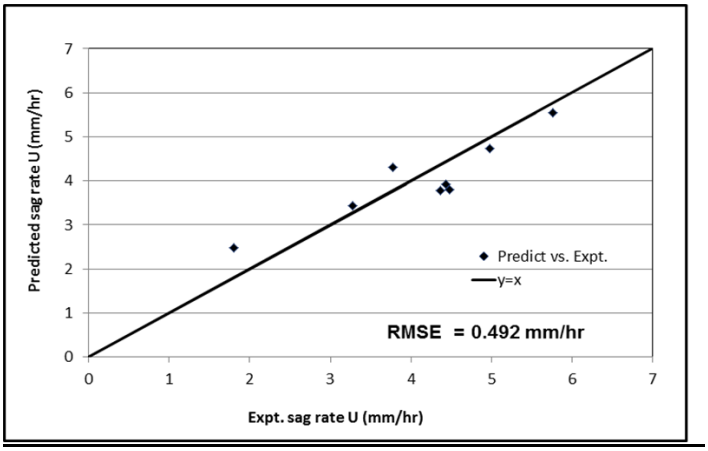

Figure 1: Plot of predicted sag rates (from Equations 4 and 5) vs. experimental sag rates (from DHAST unit)

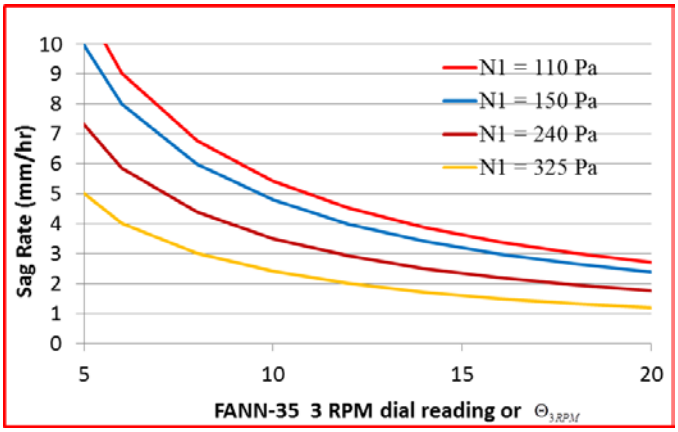

Figure 2: Plot of predicted sag rates vs. FANN 35 Viscometer $\Theta_{3RPM}\,(lb/100\,ft^2)$ at different values on N_1.

Sag Model Application of the Unseen drilling fluids

The task here was to verify whether the sag model (Equations 4 and 5) with obtained empirical constants in the earlier subsection can predict sag rates (U_{avg}) accurately for some new or unseen drilling fluids (drilling fluids that are not used for building the model parameters). This step involved formulating new drilling fluids, obtaining the rheology data (η and N_1) for these drilling fluids and then predicting the sag rate (U) using Equations 4 and 5 along with the empirical parameters established earlier.

Table 2 shows the input, i.e., the rheology data (η and N_1) summary of new drilling fluids tested for model validation. The detailed composition of these drilling fluids is shown in Appendix 1. Note that these drilling fluids also have considerable variation in terms of mud weight, i.e., barite concentration.

Table 2: Rheology data in terms of 3-RPM FANN 35 viscomenter dial reading (Θ_{3RPM}) and normal stress data (N_1) for *unseen* drilling fluids (Temperature = 150°F).

Mud No.	$\Theta_{3RPM}\,(lb/100\,ft^2)$ $[\dot{\gamma} \approx 5\,s^{-1}]$	$\|N_1\|$ (Pa) $[\dot{\gamma} \approx 5\,s^{-1}]$
Fluid-IX	6	160
Fluid-X	20	280
Fluid-XI	5	210
Fluid-XII	15	400

The rheology data (η and $|N_1|$ as obtained from Table 2 for

these drilling fluids was entered in Equations 4 and 5 which predict the sag rates (U_{avg}) using the empirical parameters established earlier. Importantly, the predicted sag rates (U_{avg}) were again reasonably accurate (RMSE = 0.59 mm/hr) when compared with the experimentally observed sag rates for these drilling fluids as shown in **Table 3.** Thus, it proves that the sag behavior of drilling fluids can be predicted by the sag model based on rheological parameters as input.

Going forward, the same sag model could be easily applied to HTHP (High Temperature High Pressure) conditions by using rheological information at these conditions.

Table 3: Predicted sag rates (from Equations 4 and 5) vs. experimental sag rates (from DHAST unit) for the *unseen* drilling fluids (fluids not used to derive α, β).

Mud No.	Expt U_{avg} (*mm/hr*)	Predicted U_{avg} (*mm/hr*)
Fluid-IX	5.08	5.96
Fluid-X	2.83	2.29
Fluid-XI	5.92	6.09
Fluid-XII	1.05	1.57

Conclusions

- Barite sag can be viewed as settling of particles in a non-Newtonian fluid.
- In addition to the drilling fluid viscosity (η), the elastic properties of the drilling fluids are observed to influence the weighting material (or barite) settling behavior in these fluids.
- The developed sag model with empirical constants could *quantitatively* predict the weighting material sedimentation (or sag) rates using the rheology data as input.

Acknowledgments

The authors would like to thank the management of Halliburton for giving appropriate permissions to publish this work.

Nomenclature

η = *fluid viscosity*
a = *particle radius*
U = *rate of sedimentation*
ρ_s = *density of the particle*
ρ_f = *density of the fluid surrounding the particles*
N_1 = *first normal stress difference*
$\dot{\gamma}$ = *shear rate*
α & β = *empirical constants in the sag model (Eq. 4)*
Θ_{3RPM} = *3-RPM FANN 35 dial readings*
PSD = *particle size distribution.*

References

1. Bern, P. et al. 2010. "Field Monitoring of Weight Material Sag". AADE-10-DF-HO-25 presented at the AADE Fluids Conference and Exhibition, April 6-7, Houston, Texas.
2. Maxey J. 2006. "Rheological Analysis of Oilfield Drilling Fluids", AADE-06-DF-HO-01, presented at AADE Fluids Conference, April 11-12, 2006, Houston, Texas.
3. Bird, R. B., W. E. Stewart and E. N. Lightfoot. 1960. *Transport Phenomena*. New York: Wiley.
4. Chhabra, R. P. 2007. *Bubbles, Drops and Particles in Non-Newtonian Fluids*. New York: Taylor & Francis.
5. Tirtaatmadja, V., P.H. T. Uhlherr and T. Sridhar. 1990. Creeping motion of spheres in fluid. *J. Non-Newtonian Fluid Mech*. **35**: 327.
6. Solomon, M. J. and S. J. Muller. 1996. Flow past a sphere in polystyrene-based Boger fluids: the effect on the drag coefficient of finite extensibility, solvent quality and polymer molecular weight. *J. Non-Newtonian Fluid Mech*., **62**: 81.
7. Boger, D. V. 1984. *Dilute Inter-Relations between Processing, Structure and Properties of Polymeric Materials.* Amsterdam: Elsevier.
8. Tonmukayakul, N., J. E. Bryant, M. S. Talbot and J.F. Morris. 2008. Dynamic and Steady Shear Properties of Reversibly Cross-Linked Guar Solutions and Their Effects on Particle Settling Behavior. Society of Rheology Conference, Monterey CA, 3-8 Aug.
9. Tonmukayakul, N., J.F. Morris and R. Prud'homme, Methods for estimating proppant transport and suspendability of viscoelastic liquids. US patent application publication No. US 2011/0219856 A1.
10. Murphy, R. et al. 2006. "Apparatus for Measuring the Dynamic Solids Settling Rates in Drilling Fluids." SPE 103088 presented at the SPE ATCE in San Antonio, 24-27 September.
11. Murphy, R. et al, 2008. "Measuring and Predicting Dynamic Sag." *SPEDC* 23 (2): 142-149.

Appendix 1: Fluid Formulations

Fluid-I (12 ppg, 65:35 OWR)

Component	Concentration, ppb
Base oil I	As required
Emulsifier	8
Lime	1.5
Fluid loss additive I	1.5
Secondary viscosifier	1.25
Cacl2 brine, (200 K)	As required **(65:35 OWR)**
Inorganic viscosifier	5
Drill solids	20
Sized Calcium carbonate	30
Barite	As required (**12 ppg**)
Primary viscosifier	3

Fluid-II (12 ppg, 65:35 OWR)

Component	Concentration, ppb
Base oil II	As required
Emulsifier	8
Lime	1.5
Fluid loss additive I	1.5
Secondary viscosifier	1.25
Cacl2 brine, (200 K)	As required **(65:35 OWR)**
Inorganic viscosifier	5
Drill solids	5
Sized Calcium carbonate	30
Barite	As required(**12 ppg**)
Primary viscosifier	3

Fluid-III (12 ppg, 70:30 OWR)

Component	Concentration, ppb
Base oil III	As required
Emulsifier	8
Lime	4
CaCl2 brine(200 K)	As required **(70:30 OWR)**
Organophilic clay viscosifier	3.5
Fluid loss additive	6
Drill solids	15
Barite	As required(**12 ppg**)

Fluid-IV (12 ppg, 65:35 OWR)

Component	Concentration, ppb
Base oil II	As required
Emulsifier	8
Lime	1.5
Fluid loss additive II	1.5
CaCl2 brine,(200 K)	As required **(65:35 OWR)**
Inorganic viscosifier	10
Drill solids	15
Sized Calcium carbonate	20
Barite	As required (**12 ppg**)
Primary viscosifier	2.5

Fluid-V (12 ppg, 75:25 OWR)

Component	Concentration, ppb
Base oil II	As required
Emulsifier	8
Lime	1.5
Fluid loss additive II	2.5
CaCl2 brine, (200 K)	As required **(75:25 OWR)**
Inorganic viscosifier	10
Drill solids	15
Sized Calcium carbonate	20
Barite	As required (**12 ppg**)
Primary viscosifier	3

Fluid-VI (12 ppg, 75:25 OWR)

Component	Concentration, ppb
Base oil II	As required
Emulsifier	8
Lime	1.5
Fluid loss additive II	4
CaCl2 brine, (200 K)	As required **(75:25 OWR)**
Inorganic viscosifier	10
Drill solids	15
Sized Calcium carbonate	20
Barite	As required (**12 ppg**)
Primary viscosifier	3

Fluid-VII (12 ppg, 65:35 OWR)

Component	Concentration, ppb
Base oil I	As required
Emulsifier	8
Lime	1.5
Fluid loss additive I	1.5
CaCl2 brine(200 K)	As required **(65:35 OWR)**
Inorganic viscosifier	2
Drill solids	10
Sized Calcium carbonate	10
Barite	As required(**12 ppg**)
Primary viscosifier	1.5

Fluid-VIII (12 ppg, 75:25 OWR)

Component	Concentration, ppb
Base oil I	As required
Emulsifier	8
Lime	1.5
Fluid loss additive II	2.5
CaCl2 brine,(200 K)	As required **(75:25 OWR)**
Inorganic viscosifier	5
Drill solids	20
Sized Calcium carbonate	20
Barite	As required (**12 ppg**)
Primary viscosifier	3

Fluid-IX (10 ppg, 75:25 OWR)

Component	Concentration, ppb
Base oil I	As required
Emulsifier	8
Lime	1.5
Fluid loss additive II	2.5
CaCl2 brine, (200 K)	As required **(75:25 OWR)**
Inorganic viscosifier	5
Drill solids	20
Sized Calcium carbonate	20
Barite	As required (**10 ppg**)
Primary viscosifier	3

Fluid-X (14.5 ppg, 75:25 OWR)

Component	Concentration, ppb
Base oil II	As required
Emulsifier	8
Lime	1.5
Fluid loss additive II	2.5
CaCl2 brine, (200 K)	As required **(75:25 OWR)**
Inorganic viscosifier	5
Drill solids	20
Sized Calcium carbonate	20
Barite	As required (**14.5 ppg**)
Primary viscosifier	3

Fluid-XI (10 ppg, 65:35 OWR)

Component	Concentration, ppb
Base oil I	As required
Emulsifier	8
Lime	1.5
Fluid loss additive I	1.5
CaCl2 brine(200 K)	As required **(65:35 OWR)**
Inorganic viscosifier	2
Drill solids	10
Sized Calcium carbonate	10
Barite	As required(**10 ppg**)
Primary viscosifier	1.5

Fluid-XII (14.5 ppg, 65:35 OWR)

Component	Concentration, ppb
Base oil I	As required
Emulsifier	8
Lime	1.5
Fluid loss additive I	1.5
CaCl2 brine,(200 K)	As required **(65:35 OWR)**
Inorganic viscosifier	2
Drill solids	10
Sized Calcium carbonate	10
Barite	As required (**14.5 ppg**)
Primary viscosifier	1.5

Appendix 2: FANN® -35 Data @150°F

RPM	Fluid-I	Fluid-II	Fluid-III	Fluid-IV	Fluid-V	Fluid-VI
600	65	47	76	75	58	86
300	42	29	52	47	35	52
200	34	23	43	37	27	40
100	25	16	32	26	19	27
6	11	7	16	14	9	12
3	10	6	15	13	8	11
PV (cp)	23	18	24	28	23	34
LSYP (lb/100 ft^2)	9	5	14	12	7	10
10 Sec/10 Min Gel Strength (lb/100 ft^2)	9/15	6/14	15/17	19/27	14/20	13/20

RPM	Fluid-VII	Fluid-VIII	Fluid-IX	Fluid-X	Fluid-XI	Fluid-XII
600	47	63	42	109	32	79
300	30	39	27	71	20	51
200	24	32	21	57	16	41
100	17	23	15	42	11	30
6	8	11	7	22	5	16
3	7	11	6	21	4	15
PV (cp)	17	24	15	38	12	28
LSYP	6	11	5	20	3	14
10 Sec/10 Min Gel Strength, (lb/100 ft^2)	7/14	12/22	8/12	26/31	5/8	18/22

Appendix 3: N_1 Data from an Advanced Rheometer

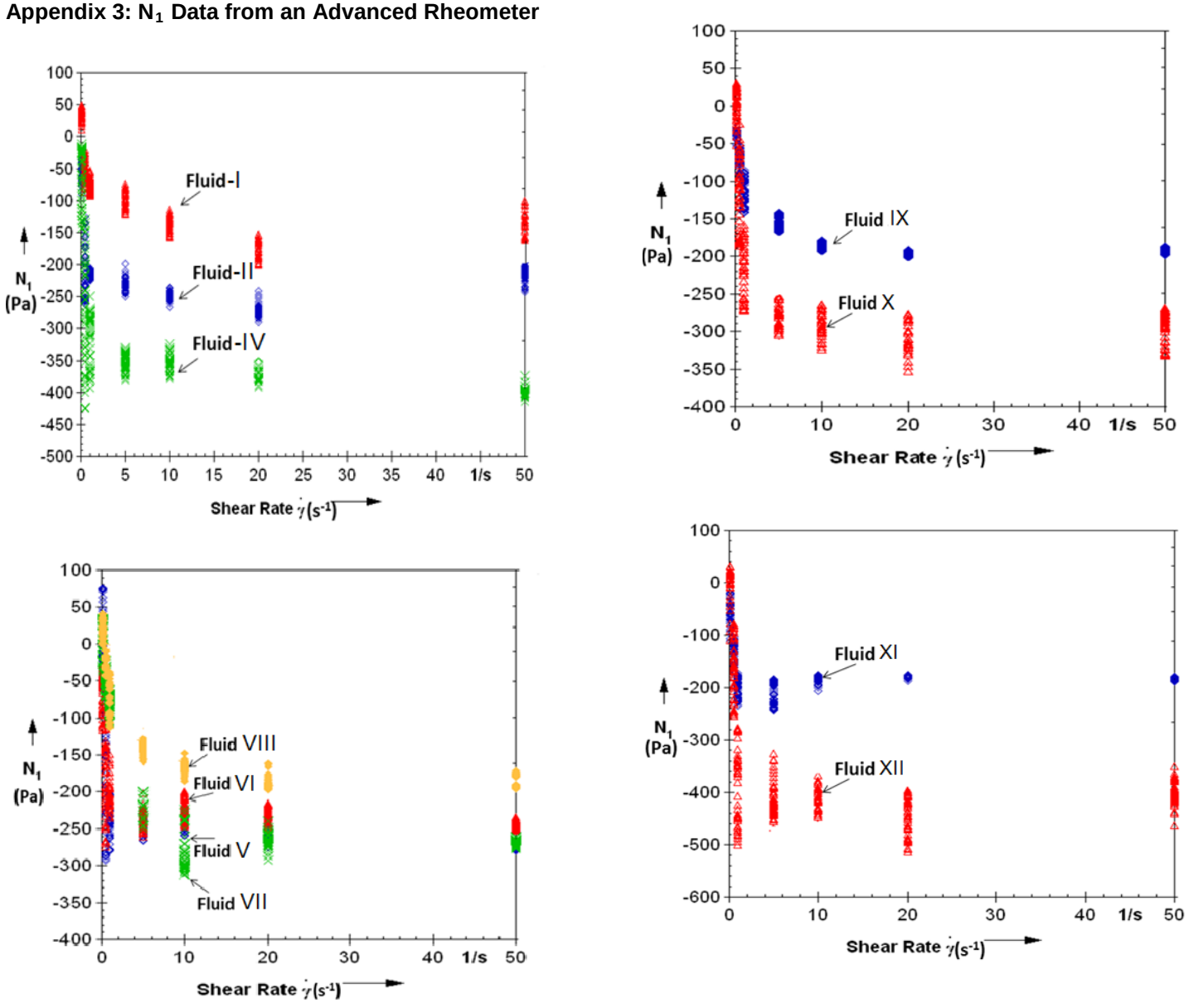

Appendix 4: Representative PSD for API Barite

Volume %

$(100 * \psi_i)$

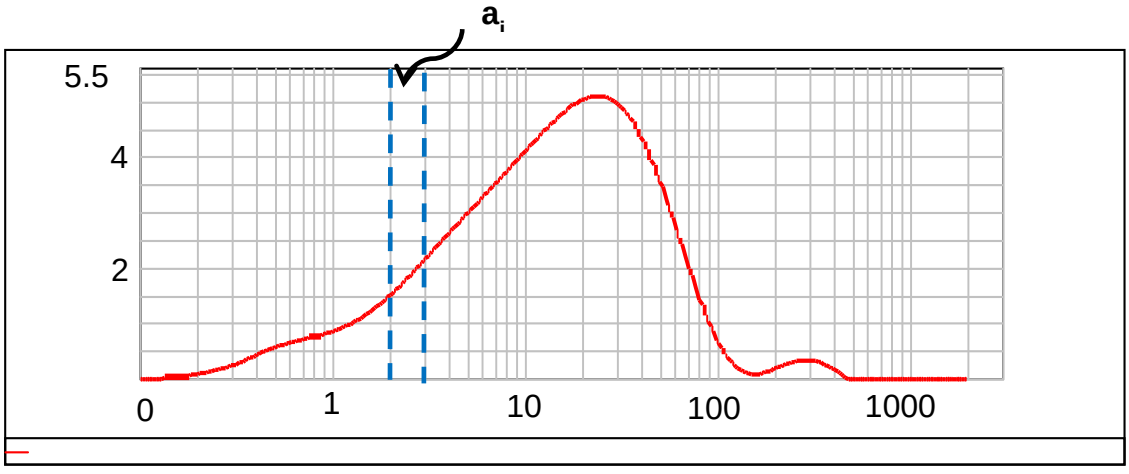

Particle size (μm)